**SUPPLEMENT**

**Table S1**. Assays to characterize ABCA3 intracellular trafficking and pumping function

| Code | Name of assay | Method | Read out | Biochemical meaning |
|---|---|---|---|---|
| A | % ER localization of ABCA3 | Co-staining immunofluorescent ABCA3$^+$ vesicles and ER markers calnexin [1, 2] | Percentage of ABCA3$^+$ vesicles colocalized with calnexin in relation to all ABCA3$^+$ vesicles | Percentage of ABCA3 localized within ER [1, 2] |
| B | N-glycosylation of ABCA3 | N-glycosylation of ABCA3-HA after digestion with endoglycosidase H (EndoH) or N-glycosidase F (PNGaseF) (Western blot) [2, 3] | Ratio of complex oligosaccharide protein (190 kDa) to hybrid oligosaccharide protein (190 kDa + 180 kDa) after EndoH digestion. | Presence of exclusive 180 kDa band after PNGaseF digestion indicates N-glycosylation of ABCA3.<br>Presence of remaining 190 kDa band after EndoH digestion demonstrates presence of complex oligosaccharide, indicating processing (N-glycosylation) in Golgi. [2-7] |
| C | % lysosomal localization of ABCA3 | Co-staining immunofluorescent ABCA3$^+$ vesicles and lysosomal marker CD63 in cells (confocal microscopy) [3] | Percentage of ABCA3$^+$ vesicles colocalized with CD63 in relation to all ABCA3$^+$ vesicles or dots | Percentage of ABCA3 processed to CD63$^+$ intracellular vesicle membrane [1-3, 6, 8-11] |

| | | | | |
|---|---|---|---|---|
| D | Proteolytic cleavage of ABCA3 | Proteolytic cleavage of ABCA3 protein (Western blot) [2] | Ratio of 170 kDa proteolytically cleaved protein band to 190 kDa non-cleaved protein band | Presence of lower band demonstrates expression of ABCA3, its transport from ER to MVB/LB [1-4, 12-15], and its proteolytic processing, likely after ABCA3 mediated lipid transport and build of LBs. |
| E | Volume of $ABCA3^+$ vesicles | Volumes of immunofluorescent $ABCA3^+$ vesicles located inside cells (confocal microscopy) [2, 13] | Volume of $ABCA3^+$ vesicles | Normal or abnormal size and structural formation of $ABCA3^+$ lysosomal compartment [1, 2, 4, 11-14, 16] |
| F | Amount of PC from recycling into $ABCA3^+$ vesicles | $ABCA3^+$ vesicles containing 1:20 TopF-PC (confocal microscopy) [17] | Fluorescence intensity of TopF-PC per $ABCA3^+$ vesicles in all $ABCA3^+$ vesicles | PC (from recycling) transport activity of $ABCA3^+$ vesicles [11, 13, 17-19] |
| G | Amount of PC from *de novo* synthesis into $ABCA3^+$ vesicles | $ABCA3^+$ vesicles containing 1:125 propargyl-choline (confocal microscopy) [16] | Fluorescence intensity of propargyl-choline per $ABCA3^+$ vesicles in all $ABCA3^+$ vesicles | PC (from *de novo* synthesis) transport activity of $ABCA3^+$ vesicles [16, 18, 19] |
| H | ATPase activity of ABCA3 | Vanadate-induced nucleotide trapping and photoaffinity labelling of ABCA3-GFP with 8-azido-[$\alpha$-32P] ATP or 8-azido-[$\alpha$-32P]ADP [3, 5, 7] | Vanadate-induced trapping analyzed by autoradiography<br>ATPase activity | ATP hydrolysis activity of ABCA3 protein [1, 3, 5, 7, 10] |

| | | | | |
|---|---|---|---|---|
| | | ATPase assay: measured as free phosphate released, compared with WT ABCA3 activity, and normalized to Western blot with anti-GFP antibody [1, 10] | | |

**Table S2.** Variants of ABCA3 included in this study.

| Variant | Model | Reference | Note |
|---|---|---|---|
| T1114S | HEK293 | [5] | |
| R288K | A549 | [10] | |
| | A549 | [2] | |
| | A549 | This paper | |
| G964D | A549 | [2] | |
| | A549 | [8] | |
| R208W | A549 | [2] | |
| E292V | A549 | [1] | |
| | A549 | [10] | |
| | A549 | [2] | |
| | HEK293 | [5] | |
| | A549 | [17] | |
| | A549 | [11] | |
| | A549 | [15] | |
| | A549 | This paper | |
| G667R | A549 | [14] | |
| N568D | A549 | [15] | |
| | A549 | [14] | |
| | HEK293, A549 | [3] | |
| | A549 | [16] | |
| | HEK293 | [7] | |
| L1580P | A549 | [14] | |

| | | | |
|---|---|---|---|
| | HEK293 | [3] | |
| | A549 | [16] | |
| F629L | A549 | [14] | |
| T1114M | A549 | [14] | |
| | HEK293 | [5] | |
| R43L | A549 | [12] | Volume of ABCA3$^+$ vesicle was not quantified. It was described that "Expression of R43L, R280C and L101P mutations had a negative effect on vesicle formation and induced a lower number of smaller compact LAMP3$^+$ vesicles", and it looked smaller than wild type at confocal image roughly.<br>PC transportation activity: uptake of C12-NBD-phospholipids PC and PE into ABCA3 vesicles in A549 cells transfected with pUB6/HA-ABCA3 vectors was studied by confocal microscopy. |
| D253H | A549 | [9] | Vesicle volume was roughly estimated from electron microscopy image |
| G1221S | HEK293, A549 | [3] | Volume of ABCA3$^+$ vesicle was not quantified. It looked similar to N568D and L1580P at confocal images, therefore absolute value was calculated as the mean value of N568D and L1580P. |
| N53Q | HEK293, A549 | [6] | Similar to wild type cells |
| R1474W | A549 | [10] | R1474W looked similar to WT, having higher absolute % ATPase activity compared to R288K<br>N-glycosylation was defined as normal, without exact value from the paper. |
| T1173R | A549 | [9] | Vesicle volume was roughly estimated from electron microscopy image |
| R295C | HEK293 | [7] | Vesicle volume was roughly estimated from electron microscopy image |
| E292K | HEK293 | [5] | |
| E690D | HEK293 | [5] | |
| T1114A | HEK293 | [5] | |
| K1388N | A549 | [13] | Defined as mis-trafficked mutation |
| | A549 | [2] | Partially mistrafficked with less proteolytically lower band (170 kDa) |

| | | | |
|---|---|---|---|
| | A549 | [17] | Able to form vesicles, but these vesicles were significantly smaller and the lipid amount within them was significantly lower than in the cells expressing ABCA3-WT |
| | A549 | [4] | Defined as functional mutation |
| S1262G | A549 | [1] | |
| D953H | A549 | This paper | |
| N140H | A549 | [1] | |
| F1077I | A549 | This paper | |
| P248S | A549 | This paper | |
| Q1045R | A549 | This paper | |
| C611R | A549 | This paper | |
| P32S | A549 | This paper | |
| E1364K | A549 | This paper | |
| G1421R | A549 | [13] | |
| | A549 | This paper | |
| A1046E | A549 | [13] | |
| | A549 | This paper | |
| V1399M | A549 | [1] | |
| | A549 | This paper | |
| G1314E | A549 | This paper | |
| F1203del | A549 | [1] | |
| R280C | A549 | [12] | Volume of $ABCA3^{+}$ vesicle was not quantified. It was described that "Expression of R43L, R280C and L101P mutations had a negative effect on vesicle formation and induced a lower number of smaller compact $LAMP3^{+}$ vesicles", and it looked smaller than wild type at confocal image roughly.<br>PC transportation activity: uptake of C12-NBD-phospholipids PC and PE into ABCA3 vesicles in A549 cells transfected with pUB6/HA-ABCA3 vectors was studied by confocal microscopy. |

| | | | |
|---|---|---|---|
| N124Q | HEK293, A549 | [6] | Immunoblot analysis of cell lysates revealed decreases in levels of ABCA3 protein expression by ~50% in single mutants of N124 and N140 and by as much as 85% when both N residues were mutated<br>Volume of $ABCA3^{+}$ vesicle was not quantified. Absolute value was roughly estimated from confocal images. |
| N140Q | HEK293, A549 | [6] | Volume of $ABCA3^{+}$ vesicle was not quantified. Absolute value was roughly estimated from confocal images. |
| G202R | A549 | This paper | |
| M760R | A549 | [13] | |
| | A549 | [13] | |
| | A549 | This paper | |
| Q215K | A549 | [13] | |
| | A549 | [13] | |
| | A549 | This paper | |
| L101P | A549 | [15] | |
| | A549 | [11] | |
| | A549 | [1] | |
| | HEK293, A549 | [3] | |
| | A549 | [12] | |
| | A549 | [10] | |
| L982P | HEK293, A549 | [3] | |
| G571R | A549 | This paper | |
| Ins1518fs | HEK293, A549 | [3] | |

| | | | |
|---|---|---|---|
| L1553P | HEK293, A549 | [3] | |
| Q1591P | HEK293, A549 | [3] | |
| E690K | HEK293 | [5] | ATPase activity （fraction of WT nt） absolute value: 2 |
| E292D | HEK293 | [5] | |
| E690R | HEK293 | [5] | |

**Table S3.** Five patients without fitting results from figure 6.

| Patient Nr. | Allele 1 | Allele 2 | Trafficking (average) | Pumping (average) | Function (average) | Function (sum) | Clinical outcome (score) | Clinical outcome | Refence |
|---|---|---|---|---|---|---|---|---|---|
| 4 | R208W | R43H | 1 | 0.655 | 0.8825 | 1.655 | 5 | Alive, lung transplant at 4 months | Wambach, JA, et al. 2014 |
| 15 | E690K | E690K | 1 | 0.625 | 0.875 | 1.625 | 5 | Alive, lung transplant at 5 months | Wambach, JA, et al. 2014 |
| 26 | K1388N | K1388N | 0.815 | 0.685 | 0.772 | 1.500 | 5 | Died at 9 weeks | Wittmann, T., et al. 2016 |
| 41 | G1421R | Q1045R | 0.525 | 0.618 | 0.574 | 1.143 | 5 | Died after 1 month | Own unpublished data |
| 46 | F1077I | F1077I | 0.911 | 0.1 | 0.708 | 1.011 | 5 | Died at 2 months | Wambach, JA, et al. 2014 |

Legends for supplemental figures

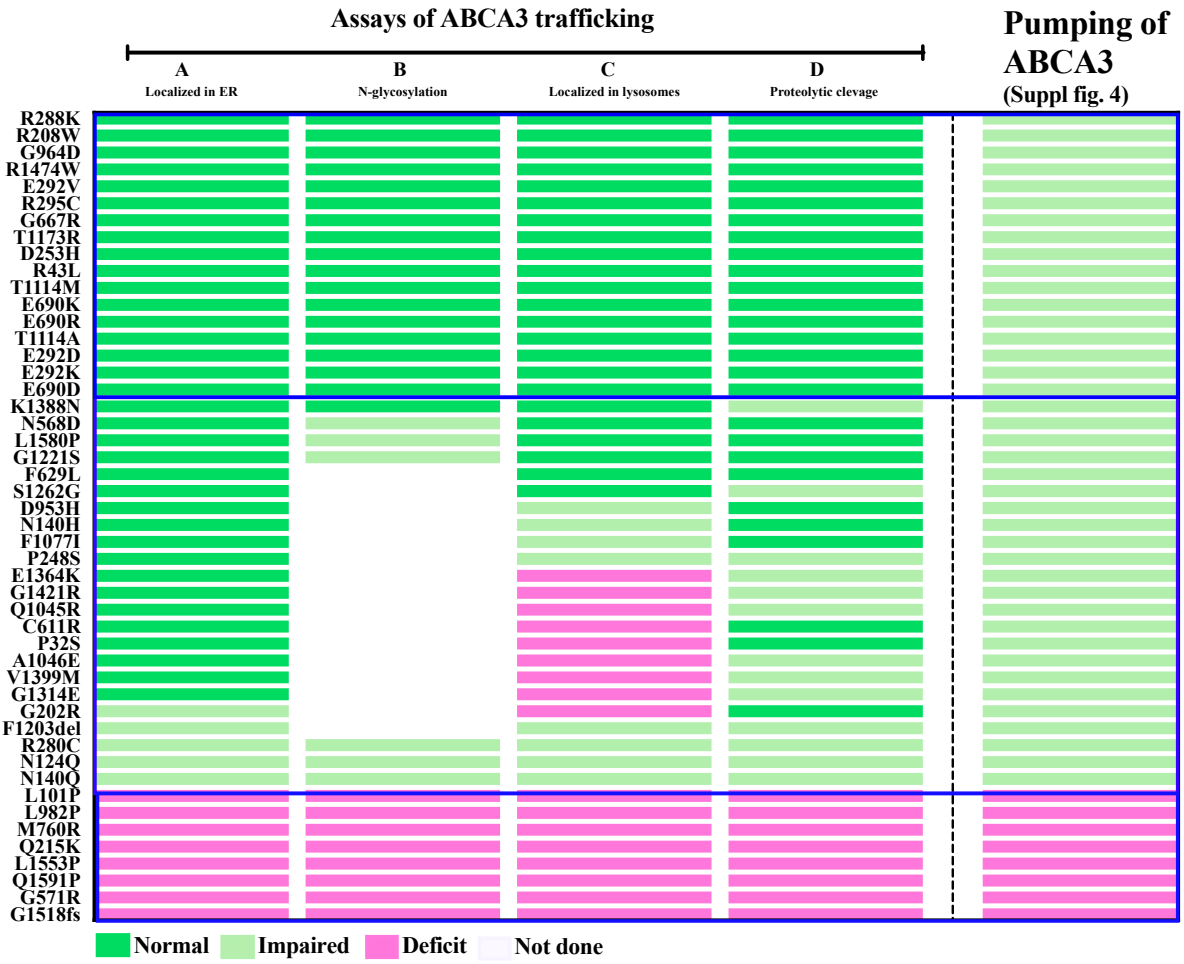


**Figure S1:** Data of disease related ABCA3 variants with assays on intracellular trafficking and function. All variants had defective ATPase activity. (a) Intracellular trafficking of ABCA3: %localized in ER (A), N-glycosylation (B), %localized in lysosomal compartments (C), proteolytic cleavage (D), and overall function of ABCA3. Dark green square indicated normal (1 ± 1 nSD), light green square indicated impaired (within 1 ± 3 nSD), purple square indicated defective (beyond 1 + 3nSD), white square indicated assays not done.

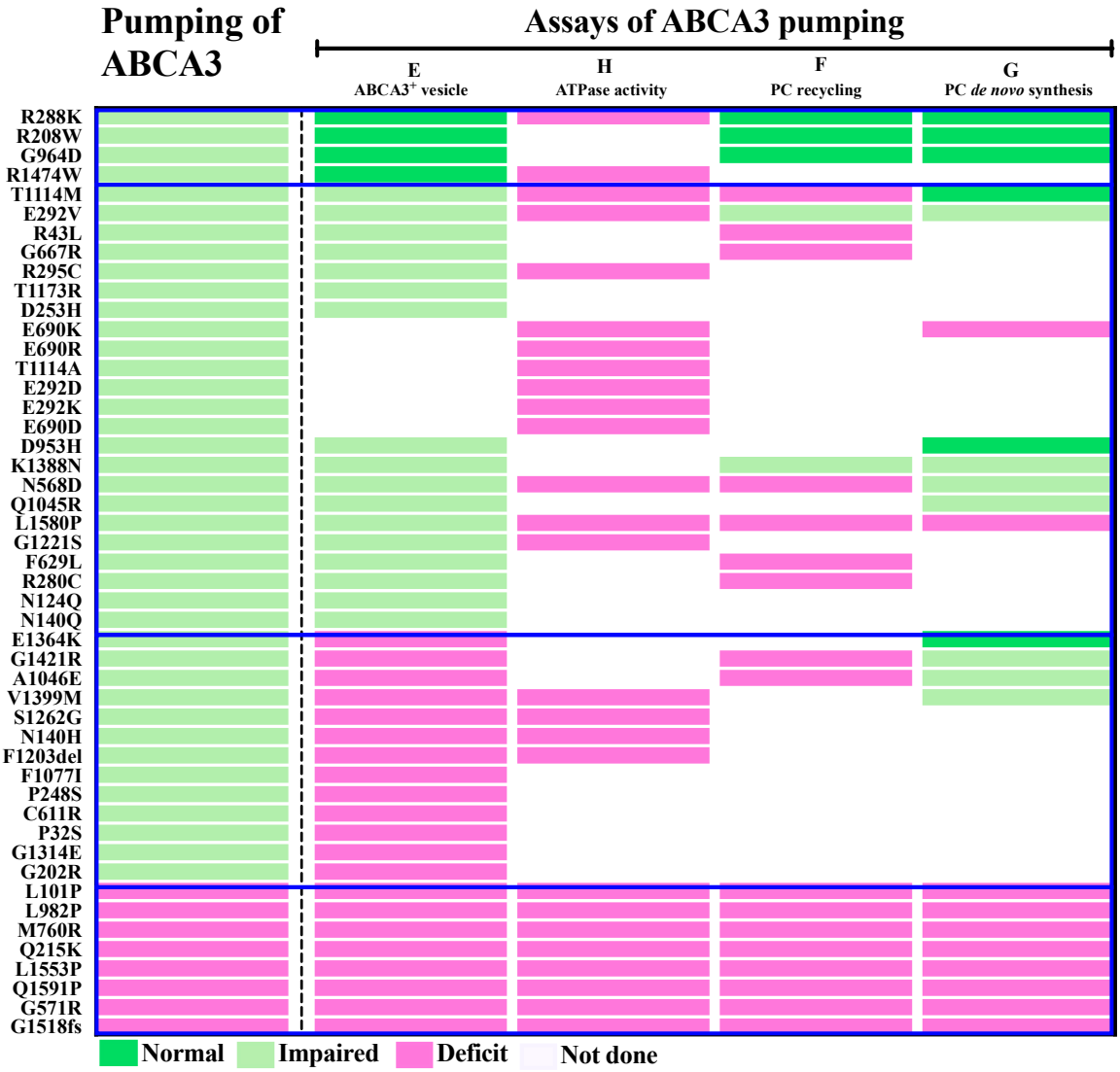


**Figure S2:** Data of disease related ABCA3 variants with assays on pumping: volume of ABCA3⁺ vesicles (E), PC from recycling into ABCA3⁺ vesicles (F), PC from *de novo* synthesis into ABCA3⁺ vesicles (G), ATPase activity of ABCA3 (H). Dark green square indicated normal (1 ± 1 nSD), light green square indicated impaired (within 1 ± 3 nSD), purple square indicated defective (beyond 1 + 3nSD), white square indicated assays not done.

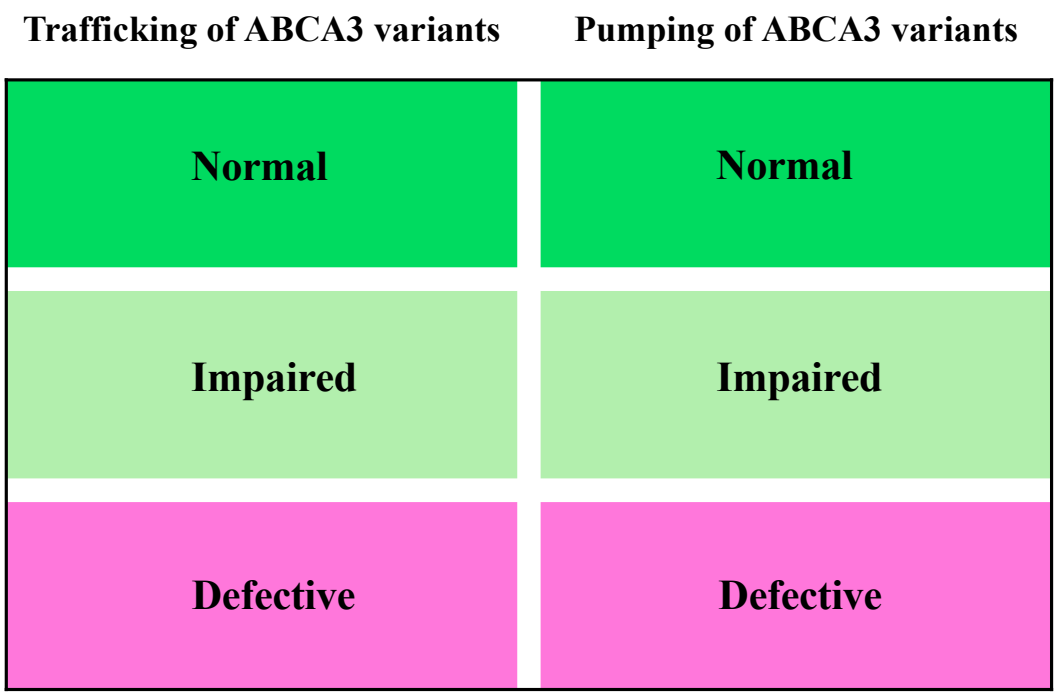


**Figure S3:** Categories of dysfunction of ABCA3 based on quantitative results of trafficking and pumping assays. Three groups of disease related ABCA3 variants were differentiated: normal trafficking but impaired pumping, impaired trafficking and impaired pumping, defective trafficking and defective pumping.

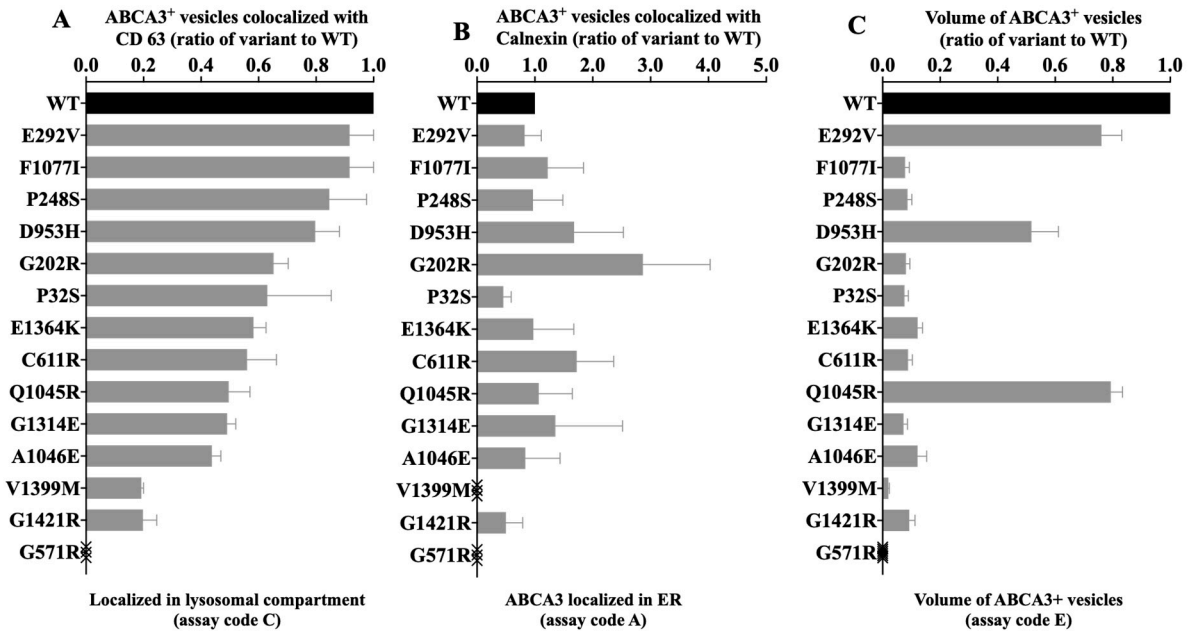


**Figure S4:** Quantitative characterization of novel ABCA3 variants: ABCA3$^+$ vesicles colocalized with CD63 (A), with calnexin (B), and mean volume of ABCA3$^+$ vesicles (C). Results were shown as Mean ± S.E.M (a - c). Cross stands for value 0.

These novel ABCA3 variants *in vitro* displayed various colocalization of ABCA3$^+$ vesicle with lysosomal compartment marker CD63 and ER marker calnexin, with significant smaller or even undatable ABCA3$^+$ vesicle. Based on the grouping method in this study, there were a variant with normal trafficking but impaired pumping (E292V), 12 variants with both impaired trafficking and pumping (F1077I, P248S, D953H, G202R, P32S, E1364K, C611R, Q1045R, G1314E, A1046E, V1399M, G1421R), and one variant with both defective trafficking and pumping (G571R).

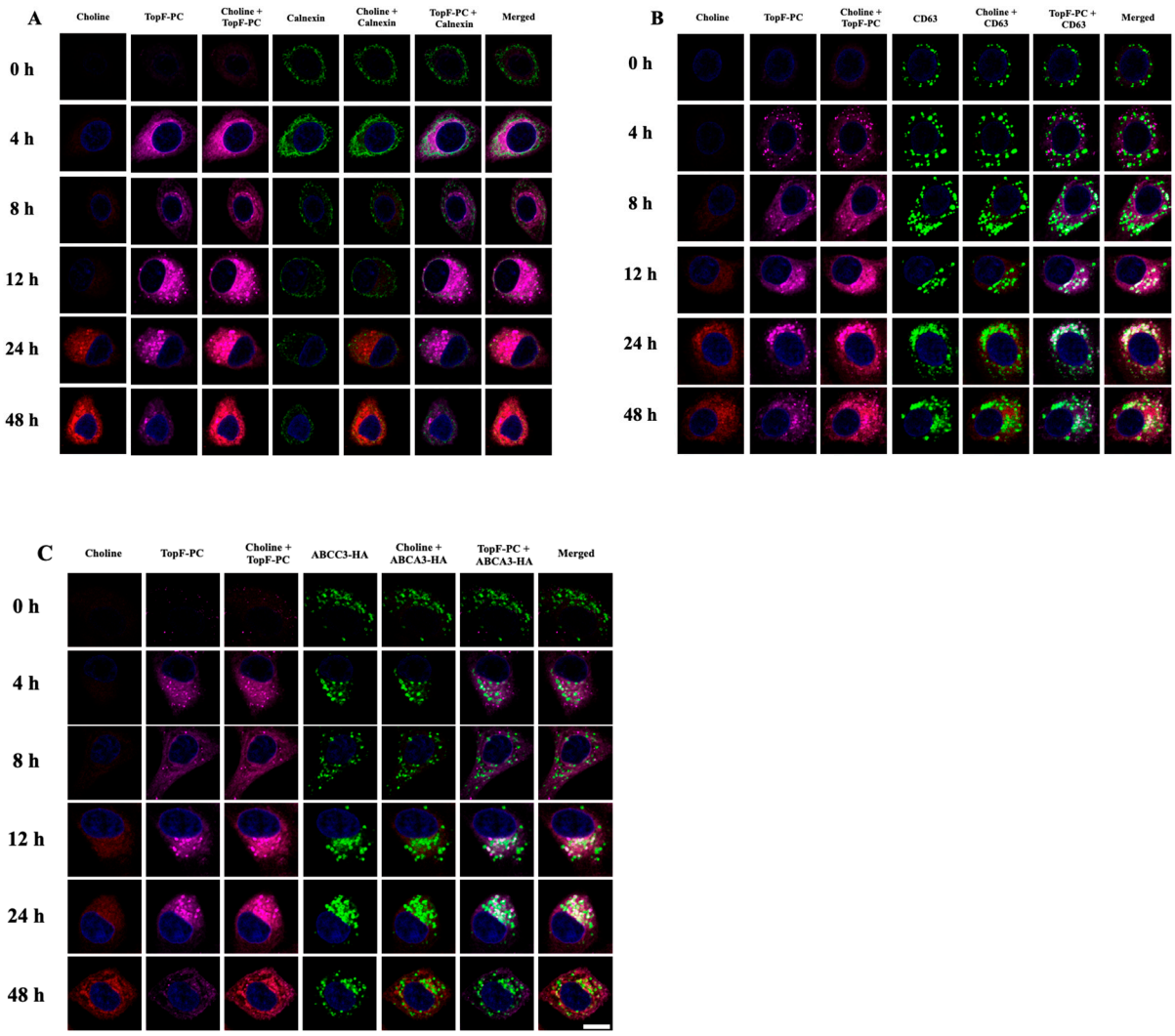


**Figure S5:** A549 cells stably express ABCA3-HA WT were incubated with 1:5 TopF-PC and 150 µM propargyl-choline for different time (0 h, 4 h, 8 h, 12 h, 24 h, 48 h) and then stained for endoplasmic reticulum (ER) marker calnexin (A), lysosomal compartment marker CD63 (B) and ABCA3-HA (C). Confocal images at different time points were taken. The results were consistent with the former experiments (100 µM propargyl-choline, n = 2; 1:20 TopF-PC, n = 2; data not shown). Scale bar: 10 µm.

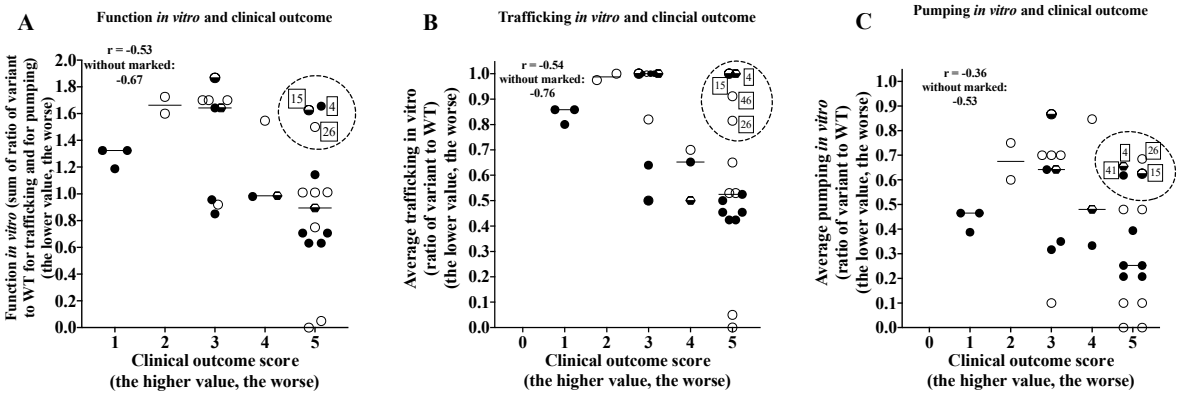


**Figure S6.** Correlation of clinical outcome in patients by score and sum value of function *in vitro* of ABCA3 variants (A), and average value of trafficking of ABCA3 variants (B), and average value of pumping of ABCA3 variants (C). Spearman r analysis was used. Solid circle: clinical outcomes of patients with compound heterozygous variants. Hollow circle: clinical outcomes of patients with homozygous variants. Semi-hollow circle: clinical outcomes of patients with homozygous variants and with lung transplanted. Semi-trapezoid: clinical outcomes of patients with compound heterozygous variants and with lung transplanted. The values without compatible results were marked with patients' ID (suppl. tab 5).

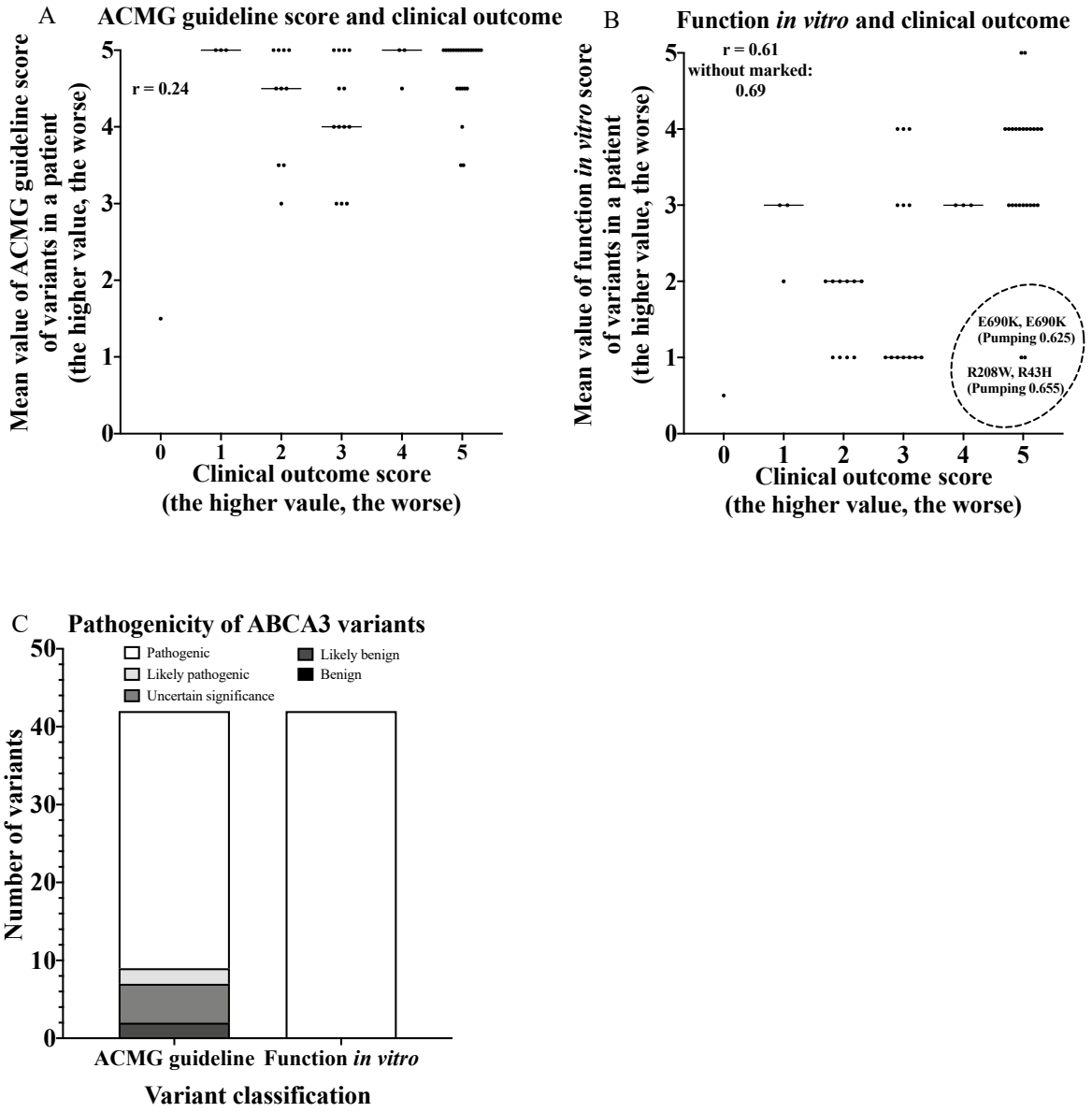


**Figure S7:** Correlation of clinical outcome and ABCA3 variants by ACMG guideline score (A), and ABCA3 variants by function *in vitro* score (B). Pathogenicity of ABCA3 variants in this study according to ACMG guideline score and function *in vitro*, respectively (C).

Function *in vitro*, ABCA3 variant with normal trafficking and normal pumping was scored as 0, with normal trafficking but impaired pumping was scored as 1, with normal trafficking but defective pumping was scored as 2, with impaired trafficking and impaired pumping was scored as 3, with impaired trafficking and defective pumping was scored as 4, and with defective trafficking and defective pumping as 5. For the variants unknown in allele 2 or not done (ND) *in vitro* experiments, assumed scoring was conducted as follows. If the clinical outcome score was 0, and ACMG guideline score < 3, then the variant function in vitro was assumed as (0). If the clinical outcome score was 1 or 2, and ACMG guideline score ≥ 3, then the variant function in vitro was assumed as (1). If the clinical outcome score was 3 or 4, and ACMG guideline score ≥ 3, then the variant function in vitro was assumed as (3). If the clinical outcome score was 5, and ACMG guideline score ≥ 3, then the variant function *in vitro* was assumed as (5).

## Reference


1. Hu, J.Y., et al., *Functional characterization of four ATP-binding cassette transporter A3 gene (ABCA3) variants.* Hum Mutat, 2020. **41**(7): p. 1298-1307.
2. Schindlbeck, U., et al., *ABCA3 missense mutations causing surfactant dysfunction disorders have distinct cellular phenotypes.* Human mutation, 2018. **39**(6): p. 841-850.
3. Matsumura, Y., et al., *Characterization and classification of ATP-binding cassette transporter ABCA3 mutants in fatal surfactant deficiency.* J Biol Chem, 2006. **281**(45): p. 34503-14.
4. Wittmann, T., et al., *Tools to explore ABCA3 mutations causing interstitial lung disease.* Pediatr Pulmonol, 2016. **51**(12): p. 1284-1294.
5. Matsumura, Y., N. Ban, and N. Inagaki, *Aberrant catalytic cycle and impaired lipid transport into intracellular vesicles in ABCA3 mutants associated with nonfatal pediatric interstitial lung disease.* Am J Physiol Lung Cell Mol Physiol, 2008. **295**(4): p. L698-707.
6. Beers, M.F., et al., *Disruption of N-linked glycosylation promotes proteasomal degradation of the human ATP-binding cassette transporter ABCA3.* Am J Physiol Lung Cell Mol Physiol, 2013. **305**(12): p. L970-80.
7. Park, S.K., et al., *Identification and characterization of a novel ABCA3 mutation.* Physiol Genomics, 2010. **40**(2): p. 94-9.
8. Campo, I., et al., *A large kindred of pulmonary fibrosis associated with a novel ABCA3 gene variant.* Respiratory Research, 2014. **15**(1): p. 43.
9. Flamein, F., et al., *Molecular and cellular characteristics of ABCA3 mutations associated with diffuse parenchymal lung diseases in children.* Hum Mol Genet, 2012. **21**(4): p. 765-75.
10. Wambach, J.A., et al., *Functional Characterization of ATP-Binding Cassette Transporter A3 Mutations from Infants with Respiratory Distress Syndrome.* Am J Respir Cell Mol Biol, 2016. **55**(5): p. 716-721.
11. Wambach, J.A., et al., *Functional Genomics of ABCA3 Variants.* Am J Respir Cell Mol Biol, 2020. **63**(4): p. 436-443.
12. Weichert, N., et al., *Some ABCA3 mutations elevate ER stress and initiate apoptosis of lung epithelial cells.* Respir Res, 2011. **12**(1): p. 4.
13. Kinting, S., et al., *Functional rescue of misfolding ABCA3 mutations by small molecular correctors.* Hum Mol Genet, 2018. **27**(6): p. 943-953.
14. Kinting, S., et al., *Potentiation of ABCA3 lipid transport function by ivacaftor and genistein.* J Cell Mol Med, 2019. **23**(8): p. 5225-5234.
15. Beers, M.F. and S. Mulugeta, *The biology of the ABCA3 lipid transporter in lung health and disease.* Cell Tissue Res, 2017. **367**(3): p. 481-493.
16. Li, Y., et al., *Metabolic labelling of choline phospholipids probes ABCA3 transport in lamellar bodies.* Biochim Biophys Acta Mol Cell Biol Lipids, 2019. **1864**(12): p. 158516.
17. Hoppner, S., et al., *Quantification of volume and lipid filling of intracellular vesicles carrying the ABCA3 transporter.* Biochim Biophys Acta Mol Cell Res, 2017. **1864**(12): p. 2330-2335.
18. Patterson, C.E., et al., *Fatty acid synthesis in the fetal lung: relationship to surfactant lipids.* Biochim Biophys Acta, 1986. **878**(1): p. 110-26.
19. Nijssen, J., et al., *Phospholipid-protein interactions in rat lung lamellar bodies.* Biochimica et Biophysica Acta (BBA)-Lipids and Lipid Metabolism, 1987. **917**(1): p. 140-147.